Influence of the generated power, measurement bandwidth, and noise level on intensity statistics of a quasi-CW Raman fiber laser

Oleg A. Gorbunov[*a,b], Srikanth Sugavanam[c], Dmitry V. Churkin[a,b,c]
[a]Institute of Automation and Electrometry SB RAS, 1 Ac. Koptyugave., Novosibirsk, 630090, Russia; [b]Novosibirsk State University, 630090, Novosibirsk, Russia; [c]Aston Institute of Photonic Technologies, Aston University, Birmingham, B4 7ET, United Kingdom;

ABSTRACT

In the present paper we numerically study instrumental impact on statistical properties of quasi-CW Raman fiber laser using a simple model of multimode laser radiation. Effects, that have the most influence, are limited electrical bandwidth of measurement equipment and noise. To check this influence, we developed a simple model of the multimode quasi-CW generation with exponential statistics (i.e. uncorrelated modes). We found that the area near zero intensity in probability density function (PDF) is strongly affected by both factors, for example both lead to formation of a negative wing of intensity distribution. But far wing slope of PDF is not affected by noise and, for moderate mismatch between optical and electrical bandwidth, is only slightly affected by bandwidth limitation. The generation spectrum often becomes broader at higher power in experiments, so the spectral/electrical bandwidth mismatch factor increases over the power that can lead to artificial dependence of the PDF slope over the power. It was also found that both effects influence the ACF background level: noise impact decreases it, while limited bandwidth leads to its increase.

Key words: statistical properties of multimode lasers, measurement equipment impact

1. INTRODUCTION

Many types of fiber lasers are usually based on long cavities having typical lengths from hundreds of meters to several kilometres. In particular, Raman fiber lasers (RFLs) have been demonstrated with a record cavity length up to 270 km[1] being promising for telecom applications as quasi-lossless transmission media[2,3]. In RFLs the typical spectral width of output radiation is about 0.1-1 nm. Thus, the output radiation of conventional RFL consists of numerous longitudinal modes, up to 10^8. Longitudinal modes interact with each other in the long nonlinear and dispersive RFL cavity, which results in stochastic radiation which can be described in the terms of wave turbulence[4-7]. As a result, the time dynamics of the RFL is complex with non-trivial statistical properties[8-11]. Other types of fiber lasers, for example, Ytterbium-doped fiber lasers, also reveal quasi-CW properties of the output radiation with non-gaussian statistics[12,13]. Possible mode correlations are reported recently in both YDFLs and short RFLs[14].

In general, statistical properties of the fiber-based system attracted a lot of attention recently in the context of the optical rogue waves[15-31]. Up to date, the extreme events statistics is observed in many optical systems including pulsed and CW pumped SC sources[16], silicon[17] and fiber[18] Raman amplifiers and lasers[10-11,19], mode-locked lasers[20,21] optical filamentation[22] and other systems. See the recent review of the field in[30-31].

Statistical properties of the radiation can reveal a lot about the mechanisms of modes interaction, modes correlations and physical mechanisms of the optical rogue wave generation. However, the experimental measurements of statistical properties are not easy to perform as the optical bandwidth is usually much larger than electrical bandwidth of the measurement equipment. This factor together with noise influence in measurement setup could affect the shape of measured intensity probability density functions and lead to wrong physical conclusions.

In the present paper, using a simple phenomenological model of the completely stochastic radiation consisting of uncorrelated modes, we study the influence of the measurement bandwidth and noise level on the statistical properties of the multimode laser radiation.

*gorbunov86oleg@gmail.com

Nonlinear Optics and Its Applications VIII; and Quantum Optics III, edited by Benjamin J. Eggleton, Alexander L. Gaeta, Neil G. R. Broderick, Alexander V. Sergienko, Arno Rauschenbeutel, Thomas Durt,
Proc. of SPIE Vol. 9136, 913613 · © 2014 SPIE · CCC code: 0277-786X/14/$18 · doi: 10.1117/12.2052296

2. NUMERICAL MODELLING BASED ON QUASI-CW MULTIMODE SYSTEM

2.1 Model of multimode laser radiation

Numerical simulation of generation process in a multimode Raman fiber laser was performed using NLSE-based model in[8-10], which shows nontrivial statistical properties of generated radiation. But NLSE-based model is not very convenient for our problem, since the complexity of the radiation temporal dynamics and statistics would make the interpretation of simulated bandwidth limitations complicated. Thus we use here a significantly simpler model being close to[32]. In this model the process of radiation formation is skipped, and its spectrum is introduced phenomenologically. Essential is that every point on frequency mesh can be treated as longitudinal laser mode (Fig. 1).

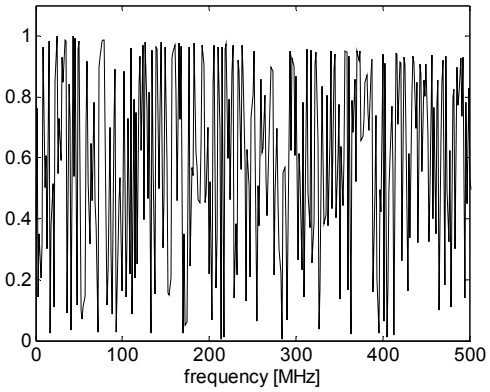

Figure 1.Mode structure, used for modelling laser radiation**.**

While using this approach we assume that modes are δ-shaped and neglect all influence of a single mode structure on entire radiation; this can be supported by the fact that in multimode lasers radiation structure is defined mainly by intermode interaction rather than single mode structure. All modes are set independent with initial phase randomly distributed in 2π interval. Amplitude of each mode is manually adjusted in such way the total spectrum envelope is agree qualitatively with experimentally measured data; quantitative agreement is, obviously, impossible with such a simple model.

The following parameters are used for modelling: frequency mesh width is 100 GHz, number of modes – 2^{16}, what corresponds to intermode interval being approximately equal to 1.53 MHz .This quantity is much less than usual number of modes in a real fiber laser, but this fact should not affect the overall results. Optical spectrum width of modelled radiation is 30 GHz by 10 dB level. Fig. 2 shows the considered spectrum and normalized intensity time dynamics, obtained from Fourier transform of signal in spectral domain.

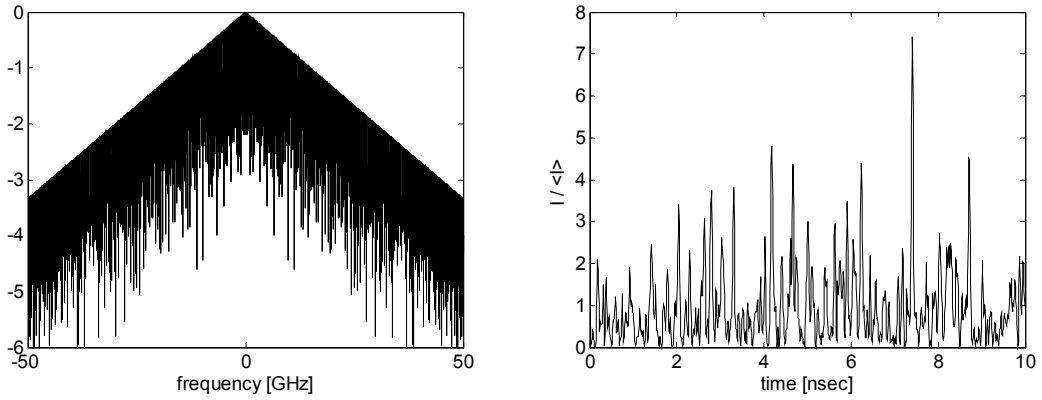

Figure 2.Full optical spectrum in logarithmic scale, used for modelling (left). Temporal dependence of intensity (right).

Stochastic nature of the temporal dynamics of the radiation is the result of random choice of initial phases; radiation can be treated as quasi-CW only. Characteristic time scale can be calculated as half-width of central peak of autocorrelation

function (ACF), given by $\frac{\langle I(t)I(t+\tau)\rangle}{\langle I^2(t)\rangle}$, and is connected with spectrum width by relation $\tau_{corr}\Delta\Omega \geq 1$, (fig. 3). The ACF level at $t >> \tau_{corr}$ is equal to 0.5, which is a common property for stochastic signal.

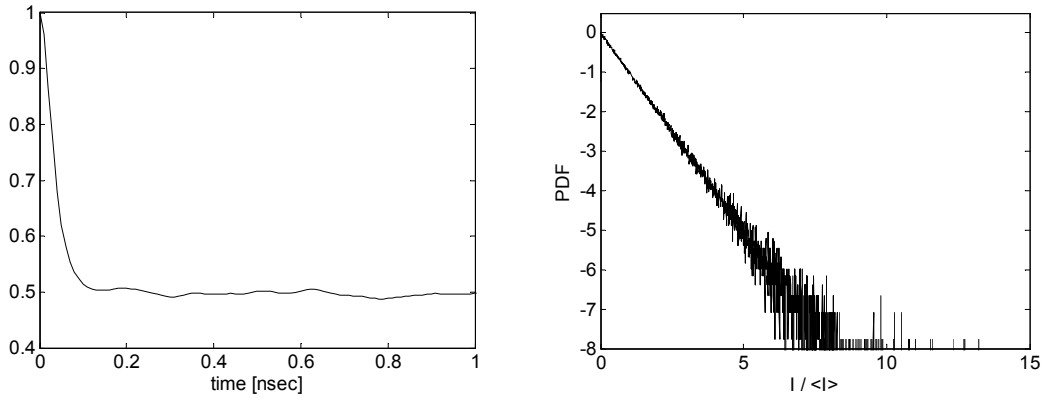

Figure 3. Intensity ACF of modelled radiation (left). Intensity PDF of modelled radiation (right).

The detailed description of a random process is achieved with probability density functions (PDFs). As central limit theorem states, the sum of a large number of independent arguments obeys the Gaussian distribution; it means that PDF is Gaussian for $E(t)$ and exponential for $I(t)$. The PDF can be obtained from the simulated trace as a histogram, built on values of intensity at different points of time mesh, and then normalized to unit area. Such a PDF, built on the base of histogram with buffer size about $3{,}3\cdot10^6$, is represented in logarithmic scale at fig. 3. The buffer size is insufficient to supress the fluctuations at the far wing of distribution, where $I > \langle I \rangle$, but apart from them PDF is exponential $\frac{1}{\langle I \rangle} e^{-\frac{I}{\langle I \rangle}}$ as expected. In our case average intensity is equal to 1, and the line can be characterized by a single value – the slope; as explained earlier, for a stochastic signal itis equal to -1.

With the validity of the numerical model verified, we now proceed to study specific cases which can affect its statistical properties.

2.2 Discussion of possible instrumental impact

In a convenient experiment[13,19] laser radiation is registered by a photodetector and then transmitted to an oscilloscope. Since the photodetector has its limited input power range, high intensity peaks may be transmitted in a nonlinear way, but this impact can be omitted by a proper choice of used power range. Other aspects usually do not affect incident radiation significantly: modern detectors generally have flat frequency response with high cut-off bandwidth and high SNR. Oscilloscopes have electrical cut-off bandwidth lower than photodetecors (up to tens of GHz, often GHz) and significant electrical noise, added to measured signal. Noise level also depends on the vertical sweep used, so to keep the SNR constant one has not only to control input power, but also use the same scale. All together these effects can significantly change original temporal and statistical characteristics of laser radiation.

For our investigation oscilloscope noise and finite electrical bandwidth were chosen, as they have the strongest impact on measurements results.

2.3 Impact of oscilloscope's noise

Noise was modelled as random function over time with Gaussian statistics, which is in qualitative agreement to typical measurement scenarios, and added to intensity; of course in frequency domain noise's uniform spectrum was also summed up with radiation RF spectrum. In average noise is usually small and for simulation is taken zero; its power is characterized by value of its fluctuations. It is convenient to characterize noise power by relation between noise distribution dispersion σ_{noise} and average input power; of course in real experiment this ratio is always significantly less

than 100%. Fig. 4 shows two different noise PDFs for a fixed input power and comparison between original intensity and the one corrupted with noise.

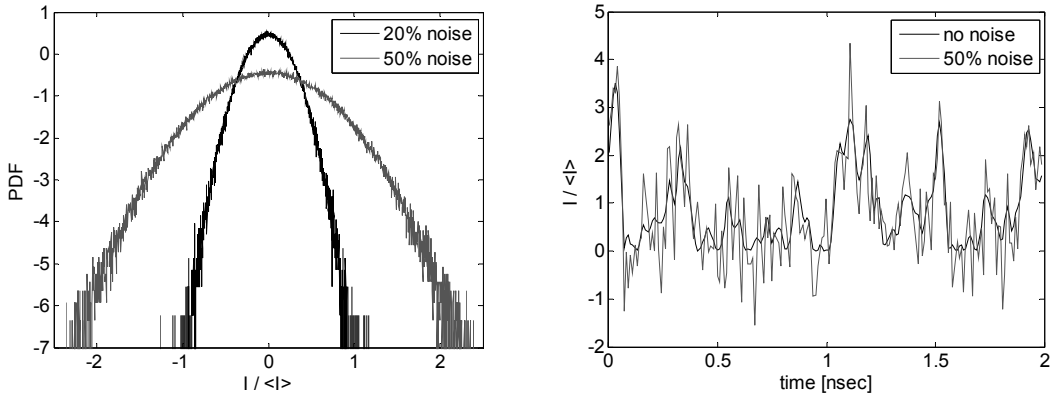

Figure 4.Noise probability distribution, used for modelling, in case of two different noise powers (left). Comparison of an intensity time trace before and after addition of 50% noise (right).

Fig. 5 performs a comparison between incident intensity PDF and two others, acquired from time dynamics traces, corrupted to variable degree. Noise corruption induces significant changes in the area near zero intensity, the PDFs acquire negative wings and distribution maximum is shifted towards positive intensities. But it is important to note that the far wings remain nearly unaffected and the slopes of the retrieved intensity PDF remain the same (fig. 5). Slope change can be observed only for SNR close to 100%.

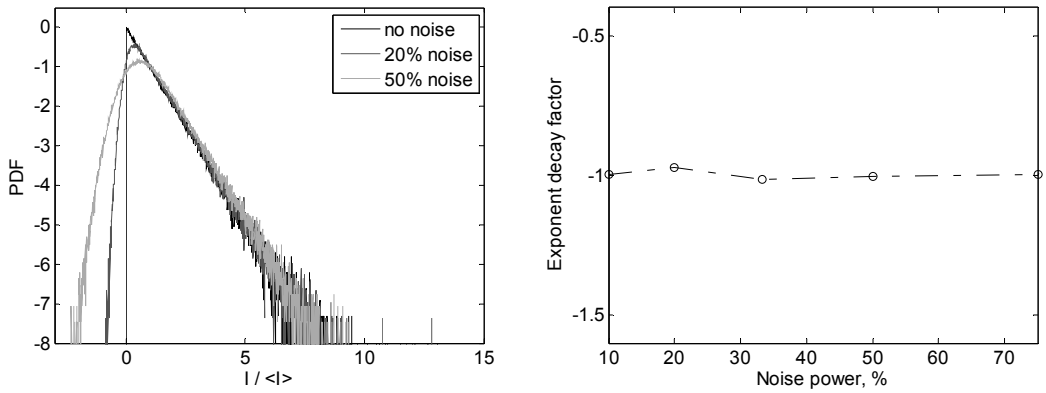

Figure 5. PDFs of original radiation and of radiation, corrupted with noise with different power (left). PDF far wing slope as function of noise power (right).

ACF is affected in two ways: its main peak becomes narrower and its background level decreases (fig. 6). Both have explanations: since noise is totally uncorrelated and symmetrical around zero, its ACF has central peak width equal to a single time step and zero level, so with increase of its influence intensity ACF shifts towards noise ACF.

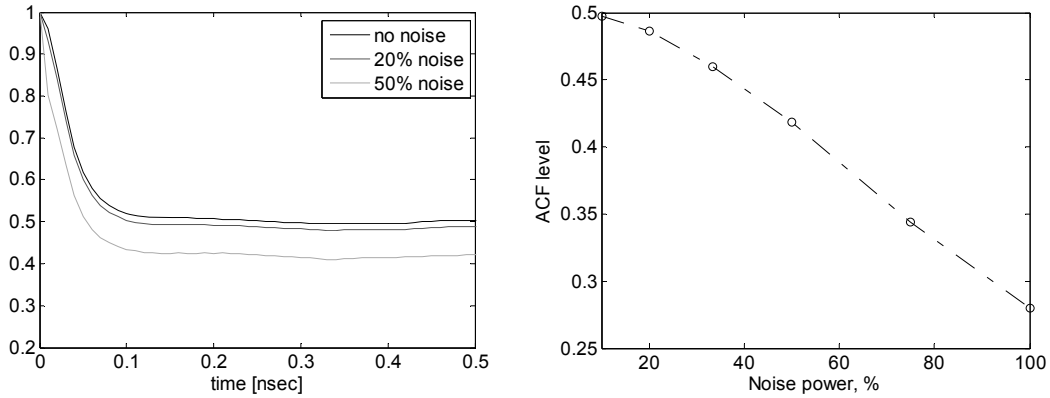

Figure 6. ACFs of original radiation and of radiation, corrupted with noise with different power (left). ACFs level as function of noise power (right).

Note that in experiments such ACF behaviour (decrease of level) can be interpreted as shift to a different generation regime. For example, in pulsed lasers the ACF level between the pulses is near zero, so any mode correlations leading to decreasing the ACF level could potenstially lead to further mode-locking. In this case misunderstanding of noise influence can lead to mistakes in understanding of underlying physics.

2.4 Impact of oscilloscope's finite bandwidth

A photodetector transmit to an oscilloscope signals proportional to incident light intensity. The oscilloscope cannot handle all frequencies of input electrical signal; all harmonics above some limit frequency are excluded from temporal dynamics. This shows the way to modelling of mentioned effect: we should cut all frequencies higher than oscilloscope limit bandwidth from intensity RF spectrum; actually we apply a rectangular spectrum filter. This, of course, does not affect the average power.

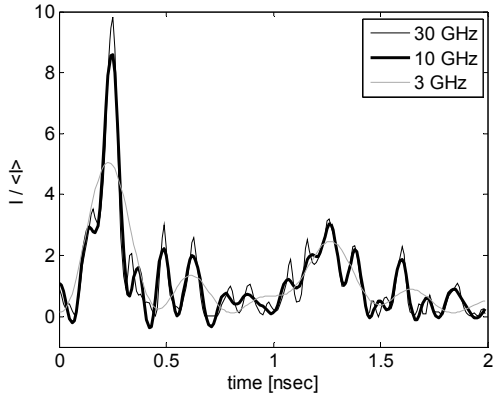

Figure 7. Intensity time dynamics for different values of limit bandwidth

Fig. 7 depicts the corresponding intensity time dynamics for different values of the filter width, which clearly shows the pronounced effect of the decreased bandwidth. Trace becomes less spiky and the increase of characteristic time can be seen even without any analysis.

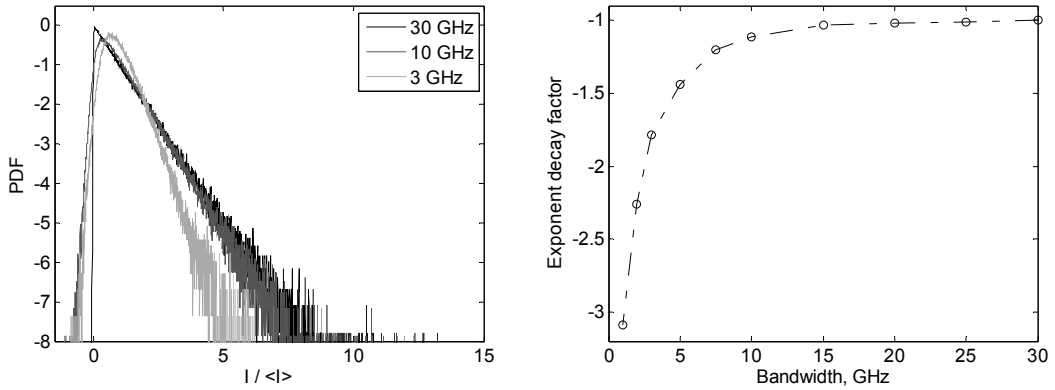

Figure 8. Intensity PDFs for different values of oscilloscope limit bandwidth (left). PDF far wing slope as function of oscilloscopelimit bandwidth (right).

Fig. 8 draws PDFs, calculated over traces with different filters applied. As it can be seen, changes are observed both at area near zero intensity and at far wing. But if shift of distribution maximum and appearance of a negative wing due to the filter function response are observed from the very beginning, the change in far wing slope is significant only for narrow oscilloscope bandwidths; slope dependence on filter width has, actually, threshold nature (fig. 8). For moderate spectral/electrical bandwidth mismatch, the effect on the PDF slope is quite marginal, but after some point the slope by absolute value starts to increase rapidly, overall PDF becomes significantly narrower and as a result intense events in radiation become highly supressed. That can be interpreted as introduction effective correlations in radiation by subtracting high frequencies from RF spectra. Note that in experiments, the generation spectrum often becomes broader at higher power, so the spectral/electrical bandwidth mismatch factor increases over the power that can lead to some dependence of the PDF slope over the power. This dependence, however, could be, at least partially, be a result of discussed effect of bandwidth mismatch influence.

Important to note that under typical experimental conditions neither noise nor bandwidth limitation does not change the PDF far wing slope significantly, we can state that experimentally observed far wings[19] are result of physical effects rather than consequence of measurement equipment limitations.

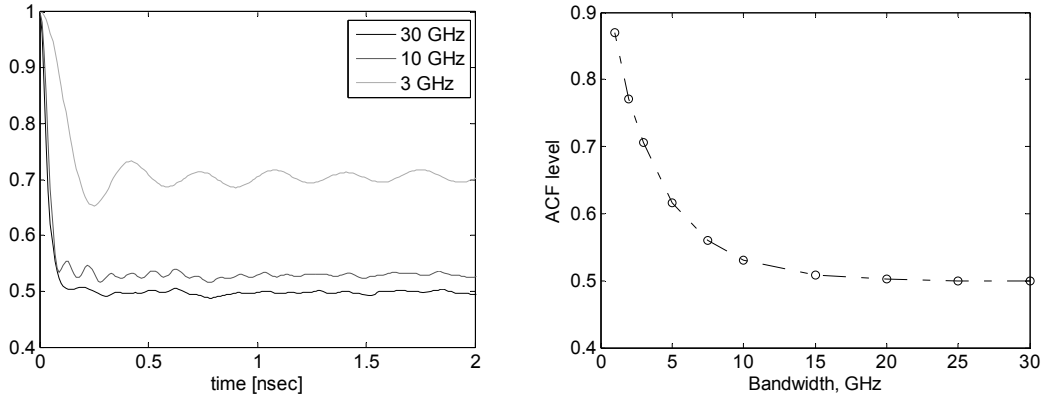

Figure 9. ACFs for different values of oscilloscope limit bandwidth (left). ACF level as function of oscilloscope limit bandwidth (right).

ACF behave itself in a similar way: apart from obvious increase of correlation time it demonstrates increase of background level, also depending on bandwidth in a threshold-like way (fig. 9). Again formally this fact can be interpreted as introduction of effective mode correlations, while for uncorrelated radiation background level must be ½.

Another effect, arising from cutting high frequencies, is appearance of ripple in ACFs. Their nature is clear: applied rectangular filter has sinc Fourier image, actually bandwidth limited detection can be revealed by the ripple signature on the ACF. But in real experiment they again can be a reason for misunderstanding.

3. CONCLUSION

Modelling of impact of measurement equipment limitations was performed using a simple model of multimode laser radiation, consisted of independent modes. Addition of noise to incident signal result in shortening of correlation time, deformation of intensity PDF zero area, and formation of a negative PDF wing. At the same time no influence on far wing PDF slope was observed even for quite high levels of noise. Effect of finite bandwidth, modelled by applying a rectangular spectral filter to radiation RF spectrum, is shown as leading to increase of correlation time, deformation of intensity PDF zero area, formation of a negative PDF wing, and appearance of ripples in ACF along with increase of its background level. Influence on far wing of PDF is threshold-like: for moderate mismatch between electrical and optical bandwidth slope nearly does not change, but from some point slope by the absolute value start to increase rapidly, which means narrowing of the entire PDF and, consequently, suppression of intense events. Experimental results, revealing far PDF wing, proved to be consequence of physical features of radiation, since as shown under typical experimental conditions neither noise, nor bandwidth limitation does not change the PDF far wing slope significantly. On the other hand, manifestation of both effects in ACF in some cases may be erroneously interpreted as evidence of physical processes.

REFERENCES

[1] S. K. Turitsyn, J. Ania-Castañón, S.A. Babin, V. Karalekas, P. Harper, D. V. Churkin, S. I. Kablukov, A. E. El-Taher, E.V. Podivilov, and V. K. Mezentsev, "270-km Ultralong Raman Fiber Laser," Phys. Rev. Lett. 103, 133901 (2009).

[2] J. D. Ania-Castanon, T. Ellingham, R. Ibbotson, X. Chen, L. Zhang, and S. Turitsyn, "Ultralong Raman Fiber Lasers as Virtually Lossless Optical Media," Phys. Rev. Lett. 96(2), 023902 (2006).

[3] M. Alcón-Camas and J. D. Ania-Castanon, "RIN transfer in 2nd-order distributed amplification with ultralong fiber lasers," Opt. Express 18(23), 23569 (2010).

[4] S. A. Babin, D. V. Churkin, A. E. Ismagulov, S. I. Kablukov, E. V. Podivilov, "Four-wave-mixing-induced turbulent spectral broadening in a long Raman fiber laser," J. Opt. Soc. Am. B, 24, 1729 (2007)

[5] Babin, S. A., Churkin, D. V., Ismagulov, A. E., Kablukov, S. I., and Podivilov, E. V., "Spectral broadening in Raman fiber lasers," Optics letters 31, 3007–3009 (2006).

[6] Babin, S. A., Churkin, D. V., Ismagulov, A. E., Kablukov, S. I., and Podivilov, E. V. "Turbulence-induced square-root broadening of the Raman fiber laser output spectrum," Optics letters 33, 633-635 (2008).

[7] S.A. Babin, V. Karalekas, E.V. Podivilov, V.K. Mezentsev, P. Harper, J. Ania-Castañón, and S.K. Turitsyn, "Turbulent broadening of optical spectra in ultralong Raman fiber lasers," Physical Review A 77, 033803 (2008).

[8] Churkin, D. V., Smirnov, S. V., and Podivilov, E. V. "Statistical properties of partially coherent cw fiber lasers," Opt. Lett. 35, 3288-3290 (2010).

[9] Randoux, S., Dalloz, N., and Suret,P. "Intracavity changes in the field statistics of Raman fiber lasers," Opt. Lett. 36, 790–792 (2011).

[10] Churkin, D. V., Gorbunov, O. A., and Smirnov, S. V. "Extreme value statistics in Raman fiber lasers," Opt. Lett. 36, 3617-3619 (2011)

[11] Churkin, D. V., and Smirnov, S. V. "Numerical modelling of spectral, temporal and statistical properties of Raman fiber lasers," Opt. Commun. 285, 2154–2160 (2012)

[12] Turitsyn, S. K., Bednyakova, A. E., Fedoruk, M. P., Latkin, A. I., Fotiadi, A. A., Kurkov, A. S., and Sholokhov,E. "Modeling of CW Yb-doped fiber lasers with highly nonlinear cavity dynamics," Opt. Express 19, 1227–1230 (2011)

[13] Bednyakova, A. E., Gorbunov, O.A., Politko, M. O., Kablukov, S. I., Smirnov, S. V., Churkin, D. V., Fedoruk,M. P. and Babin, S. A. "Generation dynamics of the narrowband Yb-doped fiber laser," Opt. Express 21, 8177-8182 (2013)

[14] Vatnik, I.D., Gorbunov, O. A., and Churkin, D. V. "Narrow-band generation and mode correlations in a short Raman fibre laser," Laser Physics 24, 025103 (2014).

[15] Solli, D. R., Ropers, C., Koonath, P., and Jalali B., "Optical Rogue Waves," Nature 450, 1054 (2007).
[16] Dudley, J. M., Genty, G., and Eggleton, B. J., "Harnessing and control of optical rogue waves in supercontinuum generation," Optics Express, 16, 3644-3651 (2008).
[17] Bourlaug, D., Fathpour, S., and Jalali, B., "Extreme Value Statistics in Silicon Photonics," IEEE Photonics J. 1, 33-39 (2009)
[18] Hammani, K., Finot, C., Dudley, G. M., and Millot, G., "Optical rogue-wave-like extreme value fluctuations in fiber Raman amplifiers," Opt. Express 16, 16467-16474 (2008)
[19] Randoux, S., and Suret, P.. "Experimental evidence of extreme value statistics in Raman fiber lasers." *Optics letters* 37, 500-502 (2012).
[20] Lecaplain, C., PhGrelu, Soto-Crespo J. M., and Akhmediev N.. "Dissipative rogue wave generation in multiple-pulsing mode-locked fiber laser." Journal of Optics 15(6), 064005 (2013).
[21] Lecaplain, C., PhGrelu, Soto-Crespo, J. M., and Akhmediev, N. "Dissipative rogue waves generated by chaotic pulse bunching in a mode-locked laser," Physical review letters 108(23), 233901 (2012).
[22] Kasparian, J., Bejot, P., Wolf, J. P., and Dudley, J.M., "Optical rogue wave statistics in laser filamentation," Opt. Express 17(14), 12070 (2009)
[23] Mussot, A., Kudlinski, A., Kolobov, M., Louvergneaux, E., Douay, M., and Taki, M., "Observation of extreme temporal events in CW-pumped supercontinuum," Opt. Express 17, 17010 (2009).
[24] Akhmediev, N., Ankiewicz, A., and Soto-Crespo, J., "Rogue waves and rational solutions of the nonlinear Schrödinger equation," Physical Review E 80, 026601 (2009).
[25] Akhmediev, N., Soto-Crespo, J. M., and Ankiewicz, A., "Extreme waves that appear from nowhere: On the nature of rogue waves," Physics Letters A 373, 2137 (2009).
[26] Dudley, J. M., Genty, G., Dias, F., Kibler, B., and Akhmediev, N., "Modulation instability, Akhmediev Breathers and continuous wave supercontinuum generation," Optics express 17, 21497 (2009).
[27] Chabchoub, Hoffmann N., and Akhmediev N., "Rogue Wave Observation in a Water Wave Tank," Physical Review Letters 106, 204502 (2011).
[28] Hammani, K., Finot, C., and Millot, G., "Emergence of extreme events in fiber-based parametric processes driven by a partially incoherent pump wave," Opt. Lett. 34, 1138 (2009)
[29] Hammani, K., Kibler, B., Finot, C., and Picozzi, A., "Emergence of rogue waves from optical turbulence," Physics Letters A 374, 3585 (2010)
[30] Akhmediev, N., Dudley, J. M., Solli, D. R., and Turitsyn, S. K.. "Recent progress in investigating optical rogue waves." Journal of Optics 15(6), 060201 (2013).
[31] Onorato, M., Residori, S., Bortolozzo, U., Montina, A., and Arecchi, F. T., "Rogue waves and their generating mechanisms in different physical contexts," Physics Reports 528(2), 47-89 (2013).
[32] Vanholsbeeck, F., Martin-Lopez, González-Herráez, M., and Coen, S., "The role of pump incoherence in continuous-wave supercontinuum generation," Opt. Express 13, 6615 (2005).